Contact models and numerical methods for metal forming processes

Patrick Chabrand

Laboratoire d'Aérodynamique et de Biomécanique du Mouvement
CNRS-Université de la Méditerranée
163 avenue de Luminy, Case 918
F-13288 Marseille

chabrand@morille.univ-mrs.fr

ABSTRACT. *The aim of the present study was first, on the macroscopic scale, to investigate the use of dynamic friction models in the analysis of tribological devices and secondly, on the microscopic scale, to analyse the shear off of two surface asperities. The effects of the macroscopic model which was found to fit a Stribeck curve will be discussed. The results will be compared with those obtained in a study performed with a constant friction coefficient. The microscopic analysis is the first step in a study of friction in terms of the plastic deformation of surface asperities. From the numerical point of view, methods used to account for the frictional contact problems in both contexts, those involving the contact occurring between rigid and deformable bodies and between two deformable bodies will be presented in detail.*

RÉSUMÉ. *L'objectif de ce travail est, à l'échelle macroscopique d'étudier l'influence de modèles de frottement variable dans l'analyse de différents essais tribologiques et à l'échelle microscopique d'analyser le cisaillement de deux aspérités de surface. Le modèle macroscopique a été identifié sur une courbe de Stribeck. Les résultats sont comparés avec ceux obtenus avec une loi de Coulomb classique à coefficient constant. L'analyse à l'échelle microscopique est la première étape d'une étude du frottement en termes de déformation plastique des aspérités de surface. Les méthodes numériques développées pour traiter le contact avec frottement aussi bien entre corps déformable et solide rigide qu'entre plusieurs corps déformables sont présentées.*

KEYWORDS: *friction, contact, variable friction coefficient, surface asperity deformation.*

MOTS-CLÉS : *frottement, contact, coefficient de frottement variable, déformation d'aspérités de surface.*

REEF – 14/2005. Finite elements in tribology, pages 323 to 337

1. Introduction

In sheet metal forming processes, the friction and lubrication crucially affect the quality of the final product in terms of the occurrence of wrinkles and necking. To improve the processes and to reduce the manufacturing costs, it is therefore necessary to closely study the friction in this context. Friction depends on many parameters which can be sub-divided into four different classes:

1. Variables associated with Stribeck curves: pressure, sliding velocities, viscosity, temperature, etc.

2. Morphology of the contacting surfaces: roughness, plastic deformation and flow of the surface asperities, etc.

3. Effects of the material and the lubricant in the contact area: the material characteristics of the tool and the sheet, the properties of the coating, lubricant and the lubrication regimes, etc.

4. Characteristics of the process: the tool geometry, clamping pressure, velocities, etc.

In this study, we dealt with the numerical analysis of the effects of all these parameters. The influence of the tool geometries and that of the process characteristics have been studied in (Chabrand *et al.*, 2005). In (Chabrand *et al.*, 1996) we described the numerical modelling of the drawbead forces required to drawn a sheet metal through a bead with a constant cross section. The aim was to determine the changes in the contact state which occurred with the drawing, and the evolution of the distribution and intensity of the contact forces.

The aim of the present investigation was two-fold. In the first part, the aim was to develop an empirical friction model based on the local contact conditions, as described by the Stribeck curve. Those curves were plotted experimentally using tribometers. To experimentally determine a friction coefficient, a metal test-piece was clamped to one of its ends and pulled out at the other end, while the central part of the test-piece was in friction contact with one or more tools. Using the measured values of the restraining forces, it was then possible to determine the friction coefficient. Depending on the geometry of the tool, this coefficient can be determined for either rounded or flat tools. The Stribeck curves (see Figure 1) were plotted for an experiment of this kind while varying the operating parameters: the pressure, lubricant viscosity, velocity of the pulling process, etc. The evolution of the friction coefficient is given as a function of the Sommerfeld parameter. Classical friction models are usually applied to problems of this kind using the global friction locally, in the finite element analysis.

The variable friction coefficient model presented here was also based on overall measurements, which were used to plot the Stribeck curve (Chertier, 1997, Chabrand and Chertier, 1996). The changes in the local coefficient were assumed to depend on the local contact conditions, satisfying on the local scale the law obtained

on the overall scale. In this part of the present study, the effects of the lubricant present between sheet and tools were not taken into account. The friction coefficient was taken to depend only on the normal nodal contact force and on the nodal sliding velocity. In (Carleer, 1997) a similar model was used to simulate square cup forming. Here a simpler test was used, focusing on the changes in several variables depending on the nodal friction coefficient. The nodal sliding velocity, contact force distribution and restraining forces were studied in particular.

In (Martinet and Chabrand, 2000), the lubricant present at the tool/sheet metal interface was studied. Hydrodynamic and elastohydrodynamic regimes were analysed using an averaged Reynolds equation. The friction coefficient was then expressed in terms of lubricant parameters such as the film thickness and viscosity and forming process parameters such as the pressure, forming speed and surface roughness.

In the second part of the study, we performed a microscopic analysis of the deformation of the surface asperities. The frictionless contact between two identical asperities face to face, moving in opposite directions was studied in particular. This part deals with the shear forces occurring at the point of contact. This is the first step in a study on the friction in terms of the plastic deformation of surface asperities. As the two asperities are assumed to be deformable, the modelling has to account for the frictional contact occurring between deformable bodies subjected to large displacements and finite deformations. To deal with multi-body contact problems, the slave/master approach is commonly used nowadays. However with this approach, the decision as to which body is the master and which the slave has to be made *a priori*. This decision generally depends on the geometry of the antagonist surfaces and on the material characteristics. The contact is taken to be the contact between a slave node and the master surface, and the numerical methods developed constrain the slave nodes so that they do not penetrate into the master body. With this approach, whether or not penetration of the master nodes into the slave body occurs is not checked and the unilateral conditions can be violated. To prevent this from occurring, various techniques based on the inversion of the roles played by the bodies to the same loading increment (Halquist *et al.*, 1985) have been developed. However with methods of this kind, the physical interpretation of the traction forces to be evaluated at each contact node is lost. We developed a symmetrical procedure for dealing with friction contact, where each body simultaneously plays the role of both the slave and the master body (Chabrand *et al.*, 2001). The contact is taken in this modelling procedure to be the contact between a slave node on each of the contact surfaces between a master segment on the antagonist surface. It is not necessary to decide *a priori* which of the two bodies will be the master and which will be the slave. A coefficient θ was introduced to weight the role played by each body and to generalize the notion of the two-pass master/slave algorithm. Depending on the value of this coefficient, it is possible to choose either the standard formulation, the symmetrical one or a formulation in which one of the bodies can be more master than slave. In addition, by introducing this coefficient into the

continuum formulation, it is possible to obtain conditions whereby each contacting body can be simultaneously master and slave. This method of formulation preserves the physical meaning of the numerical contact forces.

To solve this problem, we formulated the frictional contact problem in linear complementarity terms (Klarbring and Bjorkman, 1988). Mathematical programming methods could then be used. The displacement and contact forces, which were both unknown, were determined exactly in order to check the complementarity relations. These relations were written both on the normal components (those involved in the unilateral contact) and on the tangential ones (those involved in the friction relations). Moreover, with this method, the tangent stiffness matrix remains symmetrical, whereas penalty and Lagrange multiplier methods introduce unsymmetrical contributions. We have developed an extension of the Lemke method which gives an accurate description of the contact state, and which makes it possible to avoid having to study the stick/slip status separately, which has to be done when using a regularized approach.

In the first part of this paper, I will begin by describing the variable macroscopic friction model and I will briefly present the numerical methods used to solve the frictional contact problem which arise from this formulation. The second part is devoted to describing the frictionless shearing-off of two asperities. The method of symmetrical slave/master formulation proposed is introduced.

2. Macroscopic variable friction model

2.1. *Mechanical problem and numerical methods*

The deformable test piece was assumed to have isotropic elastoplastic behaviour involving isotropic hardening. The model adopted is characterized by an intermediate configuration based on the multiplicative decomposition of the deformation gradient F into its elastic F^e and plastic parts F^p. The behaviour of the material between the intermediate and current configurations is given by a hyperelastic response (Simo and Miehe, 1992). The intermediate configuration is updated by integrating the plastic evolutionary laws using an elastic/plastic correction method (Simo and Taylor, 1985).

The discretized form of the equilibrium equations is used to calculate the estimated incremental displacement. A modified Newton-Raphson method is used to deal with the non-linear equations arising from the finite deformations, the constitutive equations and the frictional equations.

The surface behaviour is described in terms of unilateral conditions involving friction. Various numerical methods have been used here, including both a mathematical programming method (Lemke’s method) and minimization with

projection (Gauss-Seidel, Rosen), and regularization (penalization, augmented Lagrangian) techniques (Chabrand *et al.*, 1998).

2.1.1. *Complementarity frictional contact problem*

We propose to restrict this part of the paper to dealing with the contact between a deformable body and a rigid obstacle. At each node P on the surface of the deformable body that is about to be involved in the contact, we take P_c to denote the projection of P on the surface of the rigid obstacle along its outward normal n, which is unknown *a priori*. Let Δg_N denote the gap function. At the start of the loading step, Δg_N defines the distance between the point P and P_c. We perform the following decomposition step into the normal and tangential components of the displacements (u), and the contact forces (R) :

$$u_N = u.n, \quad u_T = u - u_N n, \quad R = R_N n + R_T \qquad [1]$$

The unilateral contact conditions can then be written in terms of the relative displacement w as follows:

$$\begin{cases} w_N = \Delta u_N + \Delta g_N \\ w_N \geq 0, \quad R_N \geq 0, \quad w_N R_N = 0 \end{cases} \qquad [2]$$

As the contact condition for the tangential direction, we take Coulomb's friction law, which is written below in incremental form, in which w_T denotes the relative tangential displacement:

$$\|R_T\| \leq \mu R_N \quad \begin{cases} \|R_T\| < \mu R_N \Rightarrow w_T = 0 \\ \|R_T\| = \mu R_N \Rightarrow w_T = -\alpha R_T, \quad \alpha \geq 0 \end{cases} \qquad [3]$$

As a means of dealing with the three-dimensional case, the authors of (Klarbring and Bjorkman, 1988) have introduced a piecewise linear method approximating Coulomb's friction law. This discretization procedures makes it possible to write the friction relations as complementarity conditions and then to set the problem as a complementarity one.

In the present study, we shall restrict ourselves to a two-dimensional analysis. Two new variables, λ and ϕ , the latter of which defines the boundary of the Coulomb's cone, are introduced. The Kuhn Tucker conditions for the frictional Coulomb problem can then be written as follows:

$$\begin{cases} R_T \in C(R_N) = \{ p_T, \phi_m(p_T, R_N) \geq 0, \quad m = 1,2 \} \\ \phi_1(R_T, R_N) = -R_T + \mu R_N \\ \phi_2(R_T, R_N) = R_T + \mu R_N \\ W_T = -\lambda_1 \dfrac{\partial \phi_1}{\partial R_T} - \lambda_2 \dfrac{\partial \phi_2}{\partial R_T} \\ \lambda_m \geq 0, \quad \phi_m \geq 0, \quad \lambda_m \phi_m = 0 \quad m = 1,2 \end{cases} \qquad [4]$$

Using a condensation procedure and relations (Chabrand and Chertier, 1996), the frictional contact problem is written as a complementarity one, which can be straightforwardly solved using a pivot method such as Lemke's method (Chabrand *et al.*, 1998).

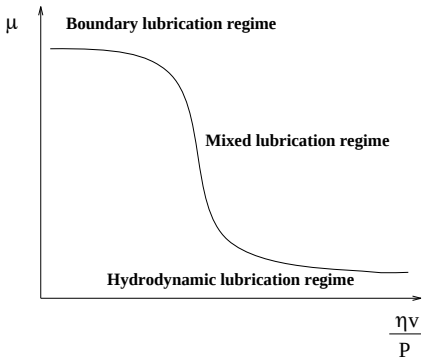

Figure 1. *Stribeck curve*

2.1.2. *Unlubricated friction model*

The effects of the lubricant viscosity, the velocity and the surface pressure on the friction coefficient can be described by a so-called Stribeck curve, as shown in Figure 1. In order to account for the change in the friction coefficient which occurs when these parameters are included in the simulation, we drew up a simple evolution equation, neglecting the lubricant.

This equation fits experimental results obtained upon varying the pressure and the speed. It yields a local friction coefficient when the local speed and the local pressure are known:

$$\begin{cases} \dfrac{v}{p} \le 8.10^{-9} \Rightarrow \mu = 0.18 \\ 8.10^{-9} < \dfrac{v}{p} < 2.10^{-7} \Rightarrow \mu = -0.063 - 0.04\, ln(\dfrac{v}{p}) \\ \dfrac{v}{p} \ge 2.10^{-7} \Rightarrow \mu = 0.04 \end{cases} \quad [5]$$

At each equilibrium equation, the contact state can be evaluated and the local value of the friction coefficient can be updated.

At each increment when the Newton-Raphson algorithm reaches convergence, a test can be carried out to check the convergence on the local friction coefficients.

The tool consists of a rigid flat die whose geometry is given in Figure 2. Because of the symmetry of the loading and that of the geometries, only half of the thickness

of the test-piece was considered here and vertical displacements were prescribed to zero on BC.

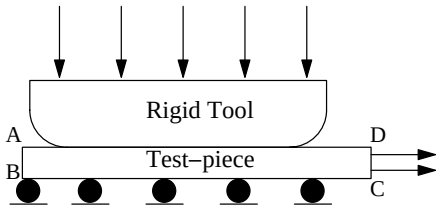

Figure 2. *Flat die test*

The unilateral conditions and the friction law were written on AD. First the tool was moved down to characterize the clamping. When the clamping force was reached, the second stage consisting of the drawing was accounted for by a prescribed horizontal incremental displacement on the right hand side of the sheet (edge DC).

In the constant case (Chabrand *et al*., 2005) first the global restraining forces increased until reaching the value μF_N. The transient effects were very short and a global Coulomb behaviour was reached after some very small horizontal displacements when the global sliding occurred.

In the variable case, the global sliding was not a steady state process. The variable friction coefficient model leads to a stick/slip regime. First before the global sliding, as in the constant case, a thinning down of the sheet occurs, due to elastic deformations. The distribution of the contact pressure on the sheet decreases until the contact is sustained by a very small area.

When the global sliding occurs, due to the decrease in the local friction coefficients, the velocity of the left hand nodes is larger than the prescribed drawing speed. The dissipated friction energy is then not sufficiently great to prevent the recovery of almost the initial sheet thickness. As the clamping is held constant and the initial thickness is recovered, the contact state is similar to the initial one. The clamping pressure is distributed almost throughout the whole sheet under the tool.

As occurs under quasi-static or dynamic analysis conditions, an oscillatory process is therefore observed, corresponding to stick/slip effects. The frequencies are in the region of the audible frequencies. The results obtained with these two methods of analysis are quantitatively different but qualitatively similar: both make it possible to characterize the phenomenon satisfactorily.

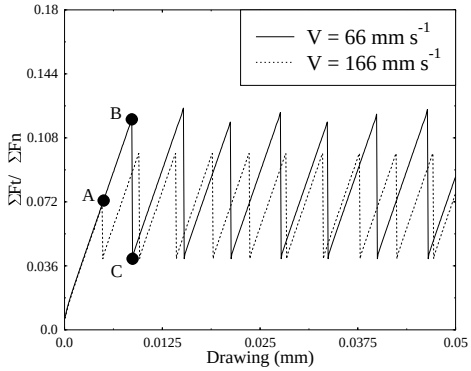

Figure 3. *Quasi-static study, global results*

Figure 3 gives, in the quasi-static case, the global ratio $\Sigma F_T/\Sigma F_N$ versus the drawing. It can be seen that with both the prescribed velocities, the stick/slip regimen is obtained. The ratio decreases with the global sliding and increases with the decrease in the contact area. Figure 4 shows the distribution of the nodal tangential velocities obtained in various loading states (see Figure 3) at the lowest prescribed velocity.

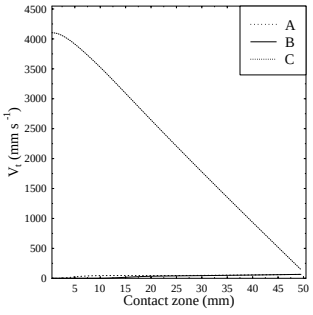

Figure 4. *Quasi static analysis, velocity distribution*

As no inertial effects are modelled in the quasi-static analysis, the global sliding is instantaneously followed by a sticking state without any plateau or any negative minimum corresponding to negative velocities, of the kind which occurs in the dynamic analysis. In the latter case, very high accelerations are observed. Figures 5-7 give the results of the dynamic analysis. Figure 5 gives the global ratio $\Sigma F_T/\Sigma F_N$ versus the drawing at the highest prescribed velocity. In this figure, four points were plotted. Point B corresponds to the time elapsing (or the increment) before global

sliding occurs. Point D is an intermediate point before a new sticking state occurs, and this is where inertial effects are observed.

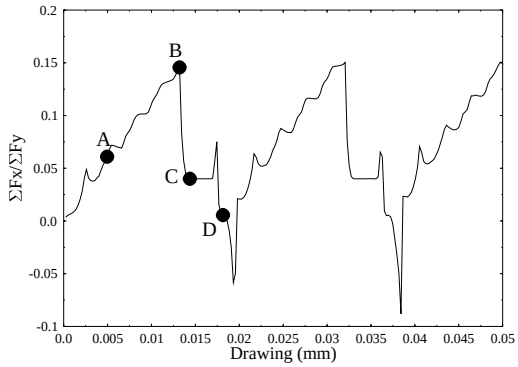

Figure 5. *Dynamic analysis, global result*

The distribution of the tangential velocities and that of the normal contact forces are plotted in Figures 6 and 7, respectively.

Before the global sliding occurs along the contact area, stick nodes are still present on the left hand side, opposite the part of the sheet where the velocities are prescribed (curves A and B Figure 6).

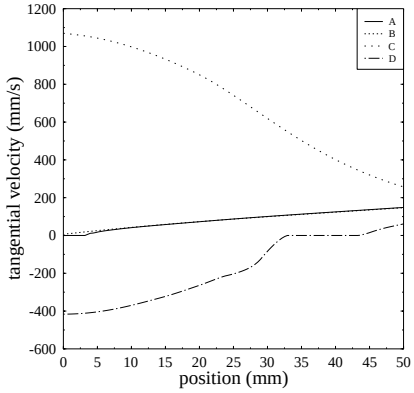

Figure 6. *Dynamic analysis, velocity distribution*

As the drawing progresses, the number of sliding nodes increases, the thickness of the sheet decreases and the clamping force is mainly supported by a decreasingly large part of the piece on the left hand side (curves A and B, Figure7).

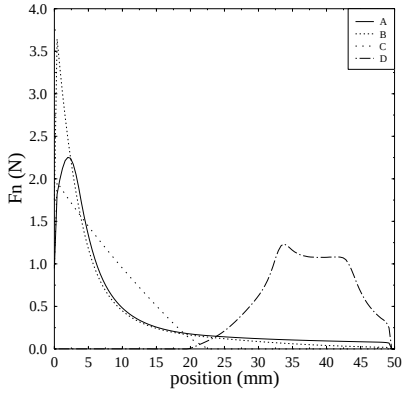

Figure 7. *Dynamic analysis, normal contact force distribution*

The velocity of the latter sliding nodes is about seven times higher than the prescribed one (curve C, Figure 6). The piece recovers its thickness and because of the inertial effects, the left hand side slides with a negative speed (curve D, Figure 7). During this transient effect, the load is supported by the right hand side of the sheet. After this, a redistribution of the thickness occurs which makes it more homogeneous and a new stick/slip regimen begins.

3. Asperity shear off

3.1. *Mechanical problem*

We consider the case of two bodies and we parametrize each surface in its reference and current configurations (Figure 8)

The potential contact surfaces are denoted $(\Gamma_c^{(i)}, i = 1,2)$ in C_0 and $(\gamma_c^{(i)} = \varphi^{(i)}(\Gamma_c^{(i)}),\ i = 1,2)$ in C_t. Each surface is simultaneously taken to be both a slave and a master surface. At time t, at a given point on one surface (which is taken to be the slave) $x^{(s)}$ (Figure 8), let us define $\overline{X}^{(m)}$ and $\overline{x}^{(m)}$ the position of the closest point on the antagonist surface in the reference and current configurations, respectively. Let $\overline{\xi}$ be the curvilinear co-ordinate solution of the following problem:

$$\overline{\xi} = \underset{\xi \in A^{(m)}}{arg\,min} \frac{1}{2} \left\| x^{(s)} - \phi^{(m)}(\xi) \right\| \qquad [6]$$

The Cauchy contact stress vector onto the slave surface is decomposed as follows:

$t^{(s)} = t_n\ n + t_g$ where index g characterizes the contravariant basis used.

In order to introduce a symmetric formulation, the virtual contact work is split into two parts weighted by a coefficient θ. The problem to be solved is then written as follows:

Problem: Find $\varphi^{(i)} : \Omega^{(i)} \times \boldsymbol{R} \to \boldsymbol{R}^n$, $t_n^{(i)} \in C_n^{(i)} = \left\{ p_n : \gamma_c^{(i)} \to \boldsymbol{R};\ p_n \geq 0 \right\}$ and $t_g^{(i)} \in C^{(i)} = \left\{ t_g^{(i)} \in \boldsymbol{R}^n,\ t_g^{(i)}.n = 0, \left\| t_g^{(i)} \right\| \leq \mu t_n^{(i)} \right\}$ for i=1,2 such that $\forall \tilde{\varphi}^{(i)} \in T_\varphi^{(i)}$ (spaces of kinematically admissible variations):

$$\sum_{i=1}^{2} \left(\int_{\omega^{(i)}} \sigma'^{i)} : \nabla^s \tilde{\varphi}^{(i)} dv^i - \int_{\omega^{(i)}} f_s^{(i)}.\tilde{\varphi}^{(i)} dv^i - \int_{\gamma_f^{(i)}} f_s^{(i)}.\tilde{\varphi}^{(i)} da_f^{(i)} \right)$$

$$-\theta \int_{\gamma_c^{(1)}} \left(t_n^{(1)} \delta d_n^{(1)} + t_{g_\alpha}^{(1)} \delta \bar{\xi}^{(\alpha)(1)} \right) da_c^{(1)} \qquad [7]$$

$$-(1-\theta) \int_{\gamma_c^{(2)}} \left(t_n^{(2)} \delta d_n^{(2)} + t_{g_\alpha}^{(2)} \delta \bar{\xi}^{(\alpha)(2)} \right) da_c^{(2)} = 0$$

$$\forall s_n^{(i)} \in C_n^{(i)} \quad \int_{\gamma_c^{(i)}} d_n^{(i)} \left(s_n^{(i)} - t_n^{(i)} \right) da_c^{(i)} \geq 0 \qquad [8]$$

$$\forall s_g^{(i)} \in C_n^{(i)} \quad \int_{\gamma_c^{(i)}} v_r^{(i)} \left(s_g^{(i)} - t_g^{(i)} \right) da_c^{(i)} \geq 0 \qquad [9]$$

Where $f_v^{(i)}$ are body forces per unit volume and $f_s^{(i)}$ are surface forces per unit area, both of which are applied to the solid $\Omega^{(i)}$, and v_r is an objective relative velocity between the slave point and the master surface. Equations [8] and [9] characterize the unilateral conditions and the Coulomb's friction law respectively, both of which are written in integral form.

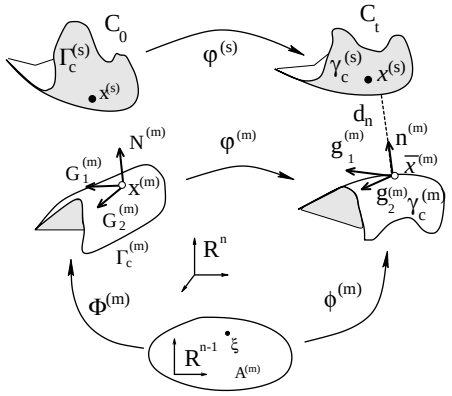

Figure 8. *Notation used for the finite deformation frictional contact problem*

To solve the discretized problem using Lemke's method, first the constraints have to be set as complementarity ones and secondly, a condensation procedure which reduces the problem to the sole variables involved in the contact has to be carried out. The first point means that the friction conditions have to be rewritten, the contact kinematic variable have to be introduced into the system to be solved and the contact forces have to be described in terms of the local contact referentials.

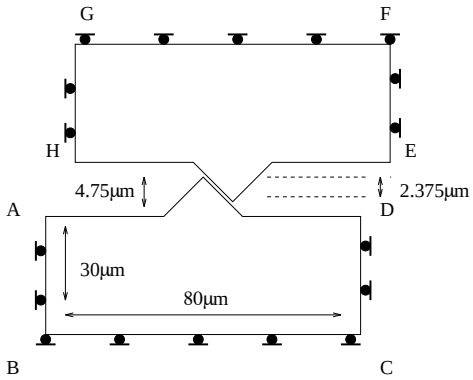

Figure 9. *Geometry of model used for shear effects*

3.2. *Asperities shear off analysis*

In this last example, we consider two asperities with identical geometries face to face moving in opposite directions (Figure 9). This part deals with the shear effects located in the contact zone.

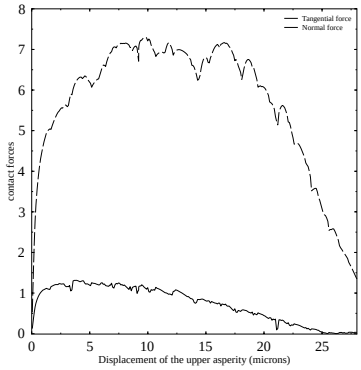

Figure 10. *Contact force evolution*

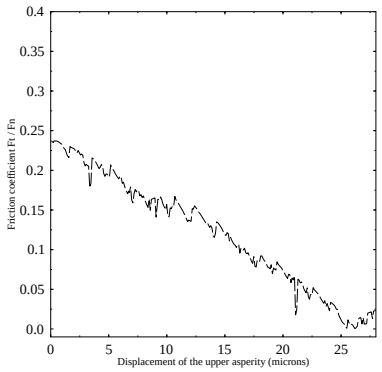

Figure 11. *Equivalent friction coefficient*

The contact is assumed to be frictionless. This is a preliminary model for characterizing the friction as a plastic shear process between asperities. The geometry of the test is given in Figure 9. Two different materials are involved. The one was an aluminium with the following material properties: $E = 70000\ MPa$, Poisson's coefficient $\nu = 0.35$. Its hardening law is given by: $\sigma_0(\bar{\varepsilon}^p) = 540(8.057\ 10^{-3} + \bar{\varepsilon}^p)^{0.28}$. The second material was a steel with the following characteristics: $E = 205900\ MPa$, $\nu = 0.3$, and its hardening law is given by: $\sigma_0(\bar{\varepsilon}^p) = 619(7.8\ 10^{-3} + \bar{\varepsilon}^p)^{0.235}$. The two bodies are meshed with Q4/P0 elements. The characteristic angle of the asperities is α= 13.36°. The meshing between the two asperities is 2.375 μm. The lower aluminium asperity remains fixed. Zero tangential displacements are prescribed on sides AB and CD, and zero vertical displacements are prescribed on BC. The upper steel asperity is moved with prescribed tangential displacements from the left to the right hand side. Figure 10 shows the evolution of the contact forces with the motion of the asperity and Figure 11 shows the changes in the ratio F_N/F_T , where F_N stands for the global normal contact force to which the lower asperity is subjected and F_T stands for the tangential force. Assuming the problem to be a frictionless one, this ratio characterizes an apparent friction coefficient. As can be observed in Figure 11, at the start of the motion, F_N/F_T is equal to the tangent to the characteristic angle of the asperities. As soon as plastic deformations occur, this coefficient decreases, reaching its minimum value when the asperity has been completely sheared off. During the process, a plastic area appears in the contact zones and increases until all the asperities have become plastic.

Lastly, Figure 12 shows various steps in the shearing process. Each arrow indicates a contact point and its length is proportional to the intensity of the contact force. Computations were carried out until the lower asperity was completely sheared. This illustrates the ability of the algorithm to deal with large changes in the

contact state from a state with high contact forces to one with very low normal forces.

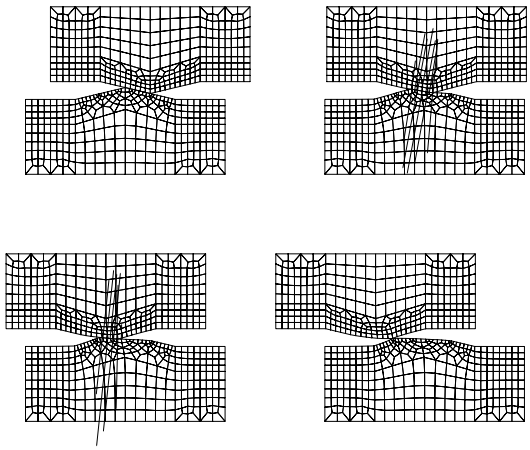

Figure 12. *Deformation of asperities at various loading steps*

4. Conclusion

The variable macroscopic model used in this study is based on local contact conditions in the absence of a lubricant film. This model differs in some respects from the classical Coulomb law with a constant global friction coefficient. In particular, an oscillatory stick/slip regimen is observed at very high frequencies. Since the clamping force is held constant, these oscillations affect the restraining forces. The evolution of the friction coefficient with respect to the local tangential velocity and normal contact force was analysed in a very simple test. Numerical modelling of this test using a variable coefficient showed the validity of this model for the contact state. To improve this approach, experimental tests will now have to be carried out and the model will be applied to more complex forming operations involving finite deformations and plasticity.

The shear off of the two asperities illustrates the ability of this symmetrical slave/master method of formulation to deal with large sliding processes. The main advantage of Lemke's method associated with the symmetrical formulation in comparison with more standard methods is that it can be used to exactly determine the two contact unknowns and then to determine the contact state without any approximation. This is extremely useful in the case of severe contact situations such as those involved in microscopic interactions. The example studied here has shown the ability of the algorithm to deal with large changes in the contact state from a state with very high contact forces to one with very law normal forces. The local analysis of the asperity deformation contributes to our understanding of contact tribology in general. The preliminary results obtained here correspond to the first

step in the modelling of friction as a plastic shear process between asperities. The numerical experiments which it is proposed to perform in further studies will involve various shapes of asperity. In particular, one of our aims will be to analyse the deep plastic effects induced by the flattening and the shearing off of asperities.

5. References

Carleer, B.D., "Finite element analysis of deep drawing", *PhD-Thesis*, University of Twente, The Netherlands, 1997.

Chabrand P., Dubois F., Raous M., "Various numerical methods for solving unilateral contact problems with friction", *Mathl Comput. Modelling*, vol. 28, 1998, p. 97-108.

Chabrand P., Dubois F., Graillet D., Boman R., Ponthot J.P., "Numerical simulation of tribological devices used as a set of benchmarks for comparing contact algorithms", *submitted for publication.*

Chabrand P., Chertier O., "Variable friction coefficient model in deep drawing", *In* T. Atlan (Ed.), *Advanced Technology of Plasticity* 1996, Colombus, Ohio, USA, p. 857-860.

Chabrand P., Dubois F., Gelin J.C., "Modelling drawbeads in sheet metal forming", *Int. J. of Mech. Sciences*, vol. 24, 1996, p. 59-77.

Chabrand P., Chertier O., Dubois F., "Complementarity methods for multibody friction problems in finite deformations", *Int. J. Numer. Meth. Engng*, vol. 51, 2001, p. 553-578.

Chertier O., Contact et frottement entre solides déformables en grandes déformations, Ph.D. Thesis, Université de la Méditerranée, 1997, Marseille.

Halquist J.O., Goudreau G.L., Benson D.J., "Sliding interfaces with contact-impact in large-scale lagrangian computations", *Comp. Meth. In Appl. Mech. And Engng*, vol. 51, 1985, p. 107-137.

Klarbring A., Bjorkman G., "A mathematical programming approach to contact problem with friction and varying contact surface", *Computers and Structures*, vol. 30, 1988, p. 1185-1198.

Martinet F., Chabrand P., "Application of ALE finite elements methods to a lubricated friction model in sheet metal forming", *Int. J. of Solids and Structures*, vol. 37, 2000, p. 4005-4031

Simo J.C., Miehe C., "Associative coupled thermoplasticity at finite strains : formulations, numerical analysis and implementations ", *Comp. Meth. In Appl. Mech. And Engng*, vol. 98, 1992, p. 41-104.

Simo J.C., Taylor R.L., "Consistent tangent operators for rate-independant elastoplasticity", *Comp. Meth. In Appl. Mech. And Engng*, vol. 48, 1985, p. 101-118.